Perceptibility of programmable softness displays using magnetorheological elastomers

Bingxu Li[1], Jaeyeon Lee[2], and Gregory J. Gerling[1]
University of Virginia[1], Ulsan National Institute of Science & Technology[2]

While often focused on our visual system, adding touch to VR/AR environments can help render more immersive, richer user experiences. One important touch percept to render is compliance, or 'softness.' Herein, we evaluate the perceptibility of soft, magnetorheological elastomers (MRE) in bare-finger interactions. Such materials can be reprogrammed to distinct states of compliance. We fabricated MRE samples over elastic moduli from 23–173 kPa and measured that small 0.25 T magnetic fields increased modulus by 10–60 kPa. MRE interfaces less and more compliant than finger skin were evaluated in discrimination experiments with and without a magnetic field. The results indicate changes in modulus of 11 kPa are required to reach a 75% threshold of discrimination, although greater differences are required when an MRE's elasticity is about the same as skin. The perceptual results with these magnetically-induced materials are similar to those with non-actuated, solid silicone-elastomers that mimic naturalistic interactions.

INTRODUCTION

The emergence of haptic interactions in a wide range of applications (e.g., VR/AR, medical simulation, surgical training, human-to-human telecommunication) demands user interfaces with natural, reconfigurable, and portable feedback. In such settings, perceptual dimensions to be recreated involve pressure, temperature, vibration, roughness, geometry, stickiness, and in particular, compliance or 'softness.' To perceive compliance, psychophysical studies indicate that we rely upon spatiotemporal patterns, or cues, in skin deformation and musculoskeletal proprioception (Srinivasan and LaMotte 1995; C. Xu, Wang, and Gerling 2021). In active, volitional touch, force-controlled movements are the most efficient and optimal for eliciting cutaneous and proprioceptive cues (Hauser and Gerling 2018; C. Xu, Wang, and Gerling 2021). This implies that the displays with solely kinesthetic cues may not sufficiently deliver a percept of softness absent cutaneous input. Indeed, when rigid plates attached to springs have been used (Heo and Lee 2017; Kim, Kim, and Lee 2016), one cannot simulate objects softer than skin, in which case the skin holds its 3D shape as it penetrates into an object's surface.

To effectively create dynamic bare-finger interactions with compliant objects, reconfigurable displays involving non-rigid surface actuation approaches have been explored. The most common approaches utilize hydraulic and pneumatic mechanisms, which use fluid or gas to deform the geometry of soft chambers and generate contact forces (Park and Wood 2013). For instance, jamming approaches control the stiffness of silicone cells, where small coffee particles dispersed in a cell respond to regulated air pressure (Menon et al. 2014; Stanley, Gwilliam, and Okamura 2013). While most hydraulic and pneumatic actuation techniques require extra instrumentation, such as an air compressor or fluid pump, other self-actuation devices utilize attraction forces between two electrodes, where a micro-chamber filled with air or fluid is deformed by internal pressure generated by electrostatic force (Leroy, Hinchet, and Shea 2020; Song et al. 2019). The limitation of this strategy is often scale, as electrostatic forces may not afford a suitable range of deformation. More recently, non-contact actuation techniques involving air flow (Lee and Lee 2016) and ultrasound (Reardon et al. 2019; Sand et al. 2015) have been proposed. Both strategies face challenges in actuating a sufficient range of forces and/or displacements to produce perceptible differences.

On the other hand, electromagnetic materials have been configured whereby the mechanical properties of fillers respond to an externally applied magnetic field. Such devices offer noiseless operation, rapid response time, and high repeatability. Ideal instantiations of haptic displays of compliance with such materials would generate a perceivable range of forces and displacements, utilize portable actuation mechanisms, and afford natural bare-finger interactions between the skin and deformable contact surfaces. Herein, we evaluate the perceptibility of several reprogrammable magnetorheological elastomer (MRE) materials in rendering discriminable percepts of compliance. Such materials have been commonly used in soft robotics as grippers as well as vibration absorbers (Deng, Gong, and Wang 2006; Hill and Snyder 2002; X. Li et al. 2021; Lu et al. 2018; Walsh and Lamancusa 1992), though not in human touch interactions. In contrast to MREs, we note that MR fluids (MRFs) have been used in human interactions (Rizzo 2013; Yang et al. 2021) and consumer displays (Ryu et al. 2015) with promise, though present drawbacks with proper sealing leading to fluid leakage and particle sedimentation. Because of their practical nature as solid substrates, MRE-based materials may render a range of compliance magnitudes and discriminable states, and thereby be useful in VR/AR touch interfaces across domains of medical stimulation, surgical training, and human-to-human telecommunication.

METHODS AND EXPERIMENTS

We investigate the ability of human participants to discriminate the compliance of MRE-based materials combining silicone rubber and iron particles. Once forming various combinations of MRE interfaces ranging from softer to stiffer than skin, a study with 10 participants evaluated their pairwise discriminability, which could be actuated up to ~10–60 kPa upon application of a magnetic field. Prior work in evaluating non-actuated, solid silicone-elastomers has shown that such ranges are discriminable.

Figure 1. (A) Magnetorheological elastomer interface (20 mm diameter, 5 mm thick) sitting atop the electromagnet (EM), (B-C) vibration observable through shape change at 2Hz with a thin MRE sample (17 mm diameter, 1 mm thick).

MRE materials principles

Magnetorheological elastomer materials are composites that embed silicone rubber with iron particles. The types and concentration of iron, magnetic particles in an MRE play an essential role in achieving the desired effect on baseline compliance and its dynamic range of actuation. Often, carbonyl iron particles (CIPs) are often used due their high magnetic permeability, fast response, and lack of hysteresis. Distinct types of silicone-elastomers can form the substrate matrix of an MRE, in specific silicone rubber, natural rubber, thermoplastic elastomer, and Polyurethane elastomer (Chen et al. 2007; Cvek et al. 2019; Wu et al. 2009; Z. Xu et al. 2020). Silicone rubber offers heat resistance, electrical insulation, and chemical stability. In particular, a silicone rubber with low shear viscosity is desirable because iron particles can be readily mixed into it in a homogeneous fashion. In this study, we explored two kinds of silicone-elastomer, a two-component silicone rubber (Ecoflex Gel and Ecoflex 00-10), and a liquid cure silicone compound (Solaris) diluted by silicone oil.

Apparatus: Fabrication of MRE-based interface samples

To create a range of distinct compliances, we fabricated MRE-based samples by varying the elasticity of silicone-elastomer and concentration of CIPs, Figure 1. The fabrication process followed two steps: 1) mixing the silicone-elastomers with fillers and 2) curing the mixture under the desired condition without alignment, Figure 2. Note that the distinct MRE samples are formed to be isotropic, i.e., with homogenous physical behaviors in each direction, which is achieved by curing them in the absence of an applied magnetic field.

In specific, the two-component silicone rubber (Ecoflex Gel) was mixed at ratio of 1:1. Next, spherical carbonyl iron particles (MiniScience, Inc. USA) with diameters of 3–10 μm were dispersed into the silicone rubber matrix of given elasticity. To minimize sedimentation, an electrical blender (12,500 rpm) was used to stir the solution thoroughly for 3 mins, Figure 2A. Then, the homogenous semi-solid mixture was placed in a vacuum chamber under 30 in-Hg pressure for 5 min to avoid porosity Figure 2B. After that, the mixture was poured into two 3-D printed circular molds and cured at 70°C for 15 mins Figure 2C. After it solidified, a 10-mm diameter, 4-mm thick sample was extracted from the first mold for subsequent modulus characterization, Figure 2D. Moreover, the MRE interface, Figure 1A, was extracted from the second mold, with exact dimensions of 20 mm diameter, 5 mm thickness. We calculated the volume fraction of each component based on its density. The concentration of CIPs was increased at increments of 5% in volume fraction until the mixture no longer formed a smooth surface, Figure 2D, right.

We generated 24 formulations with combinations of silicone-elastomers and carbonyl iron particles, Table 1 (columns 1, 2). Four silicone rubber types were employed, including Solaris (Smooth-On, Inc., USA) with 300% and 400% dilutions by silicone oil (ALPA-OIL-50, Silicone oil V50, Modulor, Germany), and Ecoflex Gel and Ecoflex 00-10 (Smooth-On, Inc., USA). As measured, they span a range of elastic modulus both more and less compliant than human skin, which lies between about 42 and 54 kPa (Miguel et al. 2015; Oprişan et al. 2016).

Apparatus: Magnetic control electronics

A single microcontroller (Teensy 3.6) controlled an electromagnet (WF-P34/25, 12 V, 200 N) in actuating an MRE sample. A transistor (TIP120) and PWM output from the microcontroller controlled the external electromagnetic field. The electromagnet consists of a cylindrical iron rod surrounded by hundreds turns of wires as adding a ferromagnetic core largely strengthens the magnetic field. By applying a magnetic field perpendicular to the surface of an MRE, it undergoes a

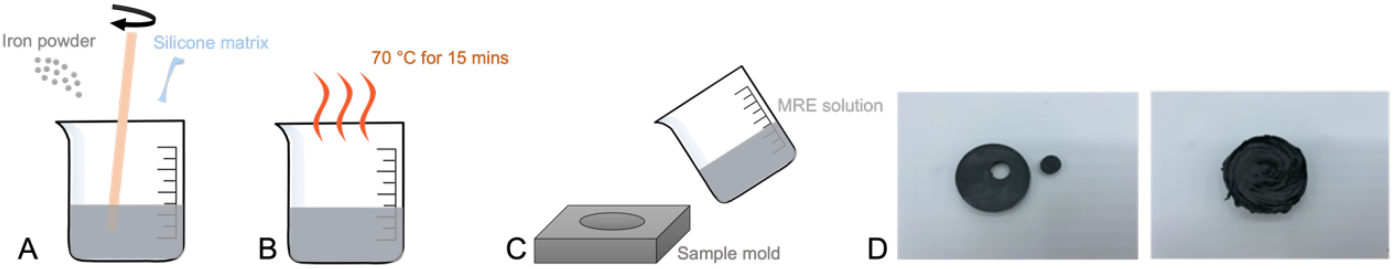

Figure 2. Step by step explanation of the MRE fabrication process. (A) Mixing two components, (B-C) Molding and curing process, (D) Left: a well-formed MRE sample with a smooth surface, made by Ecoflex Gel with 45% carbonyl iron particles (CIP). A 10 x 4 mm sample was extracted for subsequent materials characterization. Right: a poorly formed MRE sample with uneven surface, made by Ecoflex Gel with CIP 50%.

Table 1. Modulus of fabricated MRE samples. The four grey highlighted configurations were used in the human-subjects experiments.

Silicone elastomer type	CIP (%)	At 0 T (kPa)	At 0.25 T (kPa)	Effect size (kPa)
Solaris 300%	30	39.7	60.3	20.6
Solaris 300%	35	50.1	81.6	31.5
Solaris 300%	40	70.6	126.1	55.5
Solaris 300%	45	72.9	128.8	55.9
Solaris 300%	50	N/A	N/A	N/A
Solaris 400%	30	45.0	55.8	9.8
Solaris 400%	35	49.0	73.3	24.3
Solaris 400%	40	63.3	123.8	60.5
Solaris 400%	45	66.9	127.7	60.8
Solaris 400%	50	N/A	N/A	N/A
Ecoflex Gel	10	23.2	34.4	11.2
Ecoflex Gel	15	48.9	64.1	15.2
Ecoflex Gel	20	55.7	72.1	16.4
Ecoflex Gel	25	70.7	91.5	20.8
Ecoflex Gel	30	77.6	97.8	20.2
Ecoflex Gel	35	107.4	137.4	30.0
Ecoflex Gel	40	141.5	163.5	22.0
Ecoflex Gel	45	159.0	173.4	14.4
Ecoflex Gel	50	N/A	N/A	N/A
Ecoflex 00-10	10	66.5	77.7	11.2
Ecoflex 00-10	15	73.2	106.6	33.4
Ecoflex 00-10	20	88.8	126.5	37.7
Ecoflex 00-10	25	126.3	137.8	11.5
Ecoflex 00-10	30	N/A	N/A	N/A

transition in elasticity, e.g., Solaris 300% with CIP 35% modulus increased from 50 to 82 kPa with 0.25 T increase in magnetic field, Table 1. In this way, by modulating the physical form and properties of the MRE and actuating its stiffness with the electromagnet, we achieved distinct states of compliance.

Experiments: Material measurement of stiffness

The stiffness and elastic modulus of MRE samples were measured using standard uniaxial compression, by indenting a rigid plate (Gerling et al. 2018). Figure 3A illustrates force-displacement relationships two MRE configurations under two magnetic fields, where larger forces are observed with the magnetic field is set to 0.25 T. Per each substrate the error bars indicate the variance between the 3 trials performed. A linear model generated modulus by fitting a line to the first 10% of the stress and strain data, Figure 3B. Figure 3C gives elastic modulus per sample, calculated as 50.1, 81.6, 23.2, 34.4 kPa.

The complete set of the 24 MRE samples were evaluated under two magnetic fields, 0 and 0.25 T, Table 1. The absolute magnitude of their modulus ranged from 23.2 to 173.4 kPa where the modulus of each sample could be shifted from as little as 9.8 kPa to as large as 60.8 kPa.

Experiments: Human-subjects perceptual study

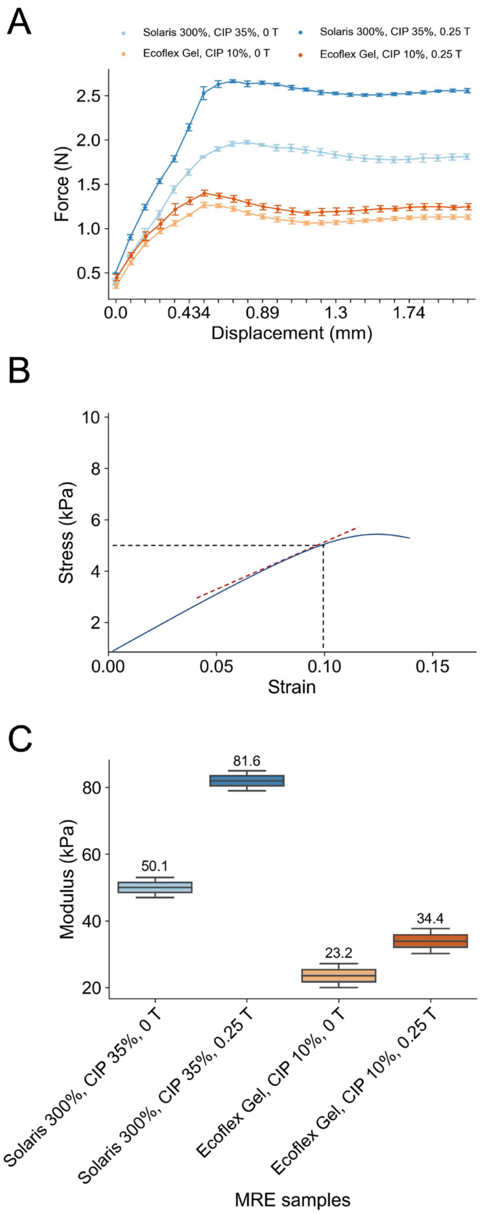

Figure 3. Stiffness and elastic modulus measurements of MRE samples. (A) Force-displacement data for two MRE configurations, where force and displacement differs between the samples, and upon the application of a 0.25 T magnetic field. (B) The stress-strain curve of the MRE sample of 50.1 kPa modulus. (C) Elastic modulus of the same four MREs, showing that a change in modulus for the Solaris sample from 50.1 to 81.6 kPa upon application of the 0.25 T magnetic field, over 3 trials, while the modulus for the Ecoflex Gel sample can be actuated from 23.2 to 34.4 kPa.

A study with 10 participants (mean age = 26.5, SD = 3) was conducted to evaluate pairwise discriminability of the MRE interfaces. As highlighted in Table 1, four pairs of MRE interfaces were selected for evaluation, which span a range of elasticities (23–82 kPa) and represent compliance values softer (23–34 kPa, Ecoflex Gel, CIP 10%) and harder (67–78 kPa, Ecoflex 00-10, CIP 10%) than the skin, as well as just slightly harder (50–82 kPa, Solaris 300%, CIP 35%) and softer (45–56 kPa, Solaris 400%, CIP 30%). For reference, the skin’s stiffness is about 42–54 kPa (Miguel et al. 2015; Oprişan et al. 2016).

MRE interfaces were placed atop the electromagnet, which was set to either 0 or 0.25 T. Each participant was seated and blindfolded to eliminate visual cues. Their index finger was guided by the proctor to the center of the interface. Participants were asked to press their finger into the interface one time and lift until it separated from the interface. Each touch interaction takes about 2 sec which consist of approximate 0.5 sec of down-up movement and 1.5 sec of exploration. The participants were asked to compare the softness of two MRE interface configurations and report which was softer. We configured each pair of interfaces at 0 T and 0.25 T in a random order, repeated five times. In total, there are 400 configurations, including four elasticity pairs, two magnetic configurations per pair, five repetitions, and ten participants.

RESULTS AND DISCUSSION

This study investigates the ability of human participants to discriminate the compliance of MRE-based materials, which combine silicone rubber and iron particles and may prove useful in VR/AR touch interfaces. In the study, where participants were asked to discriminate the compliance of MRE interfaces, the results show they could readily differentiate the 50–82 kPa pair, but not the 45–56 kPa pair, Figure 4. Discriminability for the 67–78 and 23–34 kPa pairs is near the 75% threshold of discriminability. The minimum discriminable difference in compliance is about 11 kPa, although greater differences are required when the MRE's elasticity is about the same as the skin, i.e., 45–56 kPa. In comparison, for solid elastomeric substrates, the literature shows compliance differences of 40 kPa in active touch and 28 kPa in passive touch are perceptually discriminable (B. Li, Hauser, and Gerling 2023; C. Xu, Wang, and Gerling 2021). Also, studies have shown that softness discriminability is influenced by exploration duration and time integration of sensory information (Kaim and Drewing 2011; Metzger and Drewing 2019). Moreover, distinct perceptual responses, as well as modes of skin deformation, have been observed with stiffer objects, as compared with softer objects nearer the skin's compliance (Hauser and Gerling 2018). Furthermore, we note that in this study we compared MRE interfaces to each other, but we did not compare them to solid elastomeric substrates. Further work in such regard is needed, as while the actuated elastic moduli are similar to solid substrates, there may be other perceptually discernable differences, such as relate to their viscoelastic responses.

We envision the potential use of MRE interfaces in AR/VR environments. This work evaluated these interfaces in a grounded paradigm, similar to Figure 5, lower right. Another mode of operation could be a hand or finger grounded paradigm, as in Figure 5, upper right. Indeed, such materials might be useful in human-to-human affective touch (Hauser et al. 2019), Figure 5, left. They may also be useful in virtual medical palpation training. Indeed, digital tools could help trainees familiarize and practice essential skills before real medical encounters. Current technology mainly relies on either visual recognition and/or force feedback with stick-based tasks. The MRE-based interfaces may simulate interactions with skin and other biological tissues with similar mechanical properties. Skin models for finger pad and forearm skin (42–50 kPa) and cardiac and skeletal muscles (90–110 kPa, 21–28 kPa) are feasible, Table 1, and would afford evaluating individual differences between people and normal versus disease states. Furthermore, the device might be used to simulate one's taking the pulse of a patient, as combined with the vibration functionality mode to be described below.

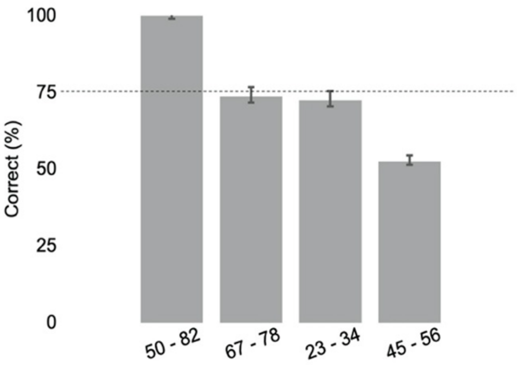

Figure 4. Results of human-subjects study. Four elasticity pairs selected from Table 1 as more compliant than skin (23–34 kPa), less compliant than skin (67–78 kPa) and overlapping with skin stiffness (50–82 and 45–56 kPa). Skin stiffness is about 42–54 kPa. Shown is a 75% level of discrimination threshold.

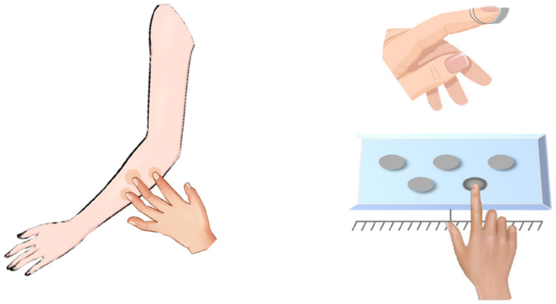

Figure 5. Human-to-human affective touch application in perceiving another's skin compliance, where an MRE-based device might be deployed in finger-grounded and surface-grounded cases.

Indeed, in addition to rendering compliance, MRE materials may also be used to render haptic vibration. Preliminarily, in work done with a thin layer of MRE with 1 mm thickness, Figure 1B, C, vibration can be delivered from 2 to 250 Hz. Without actuation, the MRE sample lays flat, as shown in Figure 1B, before areas not on top of the core are attracted to the electromagnet's surface due the ferromagnetism of the iron particles embedded in the MRE. By turning the electromagnet on and off with different frequencies, the MRE achieves unique vibratory modes. In addition to settings of the electromagnetic field, the magnitude of vibration in theory can be further controlled by two factors, the height of the core and the thickness of the MRE.

Finally, MRE-based materials, due their solid-state form, present possibilities related to shape memory where the MRE's surface can retain a contact shape. In specific, when an object is pressed into its surface in absence of magnetic field, the device surface conforms to the object's geometry. Upon introducing a magnetic field, the surface contracts and hardens rapidly towards the direction of magnetism, and as a result, the geometry of contact sustains until the magnetic field is released. Such response is rapidly onset, reversable, and highly repeatable. Shape memory functionality can also provide contact information that correlates with our perception of softness. In particular, cutaneous cues such as contact area and contact shape have been found to be associated with tactile perception and individualized and personalized calibration (B. Li and Gerling 2021; B. Li, Hauser, and Gerling 2020).

ACKNOWLEDGEMENTS

This work was supported in part by a grant from the National Science Foundation (IIS-1908115). The content is solely the responsibility of the authors and does not necessarily represent the official views of the NSF.

REFERENCES

Chen, Lin et al. 2007. “Investigation on Magnetorheological Elastomers Based on Natural Rubber.” Journal of Materials Science - J MATER SCI 42.

Cvek, Martin, Milan Kracalik, Miroslav Mrlík, and Vladimir Sedlarik. 2019. “Reprocessing of Injection-Molded Magnetorheological Elastomers Based on TPE Matrix.” Composites Part B: Engineering 172.

Deng, Hua-xia, Xing-long Gong, and Lian-hua Wang. 2006. “Development of an Adaptive Tuned Vibration Absorber with Magnetorheological Elastomer.” Smart Materials and Structures 15(5): N111–16.

Gerling, G. J. et al. 2018. “A Standard Methodology to Characterize the Intrinsic Material Properties of Compliant Test Stimuli.” IEEE Transactions on Haptics 11(4): 498–508.

Hauser, Steven C. et al. 2019. “Uncovering Human-to-Human Physical Interactions That Underlie Emotional and Affective Touch Communication.” In 2019 IEEE World Haptics Conference (WHC), 407–12.

Hauser, Steven C., and Gregory J. Gerling. 2018. “Force-Rate Cues Reduce Object Deformation Necessary to Discriminate Compliances Harder than the Skin.” IEEE Transactions on Haptics 11(2): 232–40.

Heo, Seongkook, and Geehyuk Lee. 2017. “Creating Haptic Illusion of Compliance for Tangential Force Input Using Vibrotactile Actuator.” In Adjunct Publication of the 30th Annual ACM Symposium on User Interface Software and Technology, Québec City QC Canada: ACM, 21–23.

Hill, Simon G., and Scott D. Snyder. 2002. “Design of an Adaptive Vibration Absorber to Reduce Electrical Transformer Structural Vibration.” Journal of Vibration and Acoustics 124(4): 606–11.

Kaim, Lukas, and Knut Drewing. 2011. “Exploratory Strategies in Haptic Softness Discrimination Are Tuned to Achieve High Levels of Task Performance.” IEEE Transactions on Haptics 4(4): 242–52.

Kim, Hwan, Minhwan Kim, and Woohun Lee. 2016. “HapThimble: A Wearable Haptic Device towards Usable Virtual Touch Screen.” In Proceedings of the 2016 CHI Conference on Human Factors in Computing Systems, New York, NY, USA: Association for Computing Machinery, 3694–3705.

Lee, Jaeyeon, and Geehyuk Lee. 2016. “Designing a Non-Contact Wearable Tactile Display Using Airflows.” In Proceedings of the 29th Annual Symposium on User Interface Software and Technology, UIST ’16, New York, NY, USA: Association for Computing Machinery, 183–94.

Leroy, Edouard, Ronan Hinchet, and Herbert Shea. 2020. “Multimode Hydraulically Amplified Electrostatic Actuators for Wearable Haptics.” Advanced Materials 32(36): 2002564.

Li, Bingxu, and Gregory J. Gerling. 2021. “Individual Differences Impacting Skin Deformation and Tactile Discrimination with Compliant Elastic Surfaces.” In 2021 IEEE World Haptics Conference (WHC), 721–26.

Li, Bingxu, Steven C. Hauser, and Gregory J. Gerling. 2020. “Identifying 3-D Spatiotemporal Skin Deformation Cues Evoked in Interacting with Compliant Elastic Surfaces.” In 2020 IEEE Haptics Symposium (HAPTICS), 35–40.

Li, Bingxu, Steven C. Hauser, and Gregory J. Gerling. 2023. “Faster Indentation Influences Skin Deformation to Reduce Tactile Discriminability of Compliant Objects.” IEEE Transactions on Haptics 16(2): pp. 215-227.

Li, Xianghao et al. 2021. “A Magneto-Active Soft Gripper with Adaptive and Controllable Motion.” Smart Materials and Structures 30(1): 015024.

Lu, Haojian et al. 2018. “A Bioinspired Multilegged Soft Millirobot That Functions in Both Dry and Wet Conditions.” Nature Communications 9(1): 3944.

Menon, Samir et al. 2014. “Mapping Stiffness Perception in the Brain with an FMRI-Compatible Particle-Jamming Haptic Interface.” Annual International Conference of the IEEE Engineering in Medicine and Biology Society. IEEE Engineering in Medicine and Biology Society. Annual International Conference 2014: 2051–56.

Metzger, Anna, and Knut Drewing. 2019. “Effects of Stimulus Exploration Length and Time on the Integration of Information in Haptic Softness Discrimination.” IEEE Transactions on Haptics 12(4): 451–60.

Miguel, E. et al. 2015. “Characterization of Nonlinear Finger Pad Mechanics for Tactile Rendering.” In 2015 IEEE World Haptics Conference (WHC), 63–68.

Oprişan, C et al. 2016. “Experimental Determination of the Young’s Modulus for the Fingers with Application in Prehension Systems for Small Cylindrical Objects.” IOP Conference Series: Materials Science and Engineering 147: 012058.

Park, Yong-Lae, and Robert J. Wood. 2013. “Smart Pneumatic Artificial Muscle Actuator with Embedded Microfluidic Sensing.” In 2013 IEEE SENSORS, 1–4.

Reardon, Gregory et al. 2019. “Cutaneous Wave Propagation Shapes Tactile Motion: Evidence from Air-Coupled Ultrasound.” In 2019 IEEE World Haptics Conference (WHC), 628–33.

Rizzo, Rocco. 2013. “A Permanent-Magnet Exciter for Magneto-Rheological Fluid-Based Haptic Interfaces.” IEEE Transactions on Magnetics 49(4): 1390–1401.

Ryu, Semin et al. 2015. “Design, Simulation, and Testing of a Magnetorheological Fluid–Based Haptic Actuator for Mobile Applications.” Journal of Intelligent Material Systems and Structures 26(13): 1670–78.

Sand, Antti et al. 2015. “Head-Mounted Display with Mid-Air Tactile Feedback.” In Proceedings of the 21st ACM Symposium on Virtual Reality Software and Technology, VRST ’15, New York, NY, USA: Association for Computing Machinery, 51–58.

Song, Kahye et al. 2019. “Pneumatic Actuator and Flexible Piezoelectric Sensor for Soft Virtual Reality Glove System.” Scientific Reports 9(1): 8988.

Srinivasan, Mandayam A, and Robert H LaMotte. 1995. “Tactual Discrimination of Softness.” Journal of Neurophysiology 73(1): 88–101.

Stanley, Andrew A., James C. Gwilliam, and Allison M. Okamura. 2013. “Haptic Jamming: A Deformable Geometry, Variable Stiffness Tactile Display Using Pneumatics and Particle Jamming.” In 2013 World Haptics Conference (WHC), 25–30.

Walsh, P. L., and J. S. Lamancusa. 1992. “A Variable Stiffness Vibration Absorber for Minimization of Transient Vibrations.” Journal of Sound and Vibration 158(2): 195–211.

Wu, Jinkui et al. 2009. “Preparation and Characterization of Isotropic Polyurethane Magnetorheological Elastomer Through In Situ Polymerization.” Journal of Applied Polymer Science 114: 901–10.

Xu, Chang, Yuxiang Wang, and Gregory J. Gerling. 2021. “An Elasticity-Curvature Illusion Decouples Cutaneous and Proprioceptive Cues in Active Exploration of Soft Objects.” PLOS Computational Biology 17(3): e1008848.

Xu, Zhiqiang et al. 2020. “Study on Movement Mechanism of Magnetic Particles in Silicone Rubber-Based Magnetorheological Elastomers with Viscosity Change.” Journal of Magnetism and Magnetic Materials 494: 165793.

Yang, Tae-Heon et al. 2021. “Magnetorheological Fluid Haptic Shoes for Walking in VR.” IEEE Transactions on Haptics 14(1): 83–94.